© 2014. Published by The Company of Biologists Ltd | Development (2014) 141, 1780-1788 doi:10.1242/dev.102111

RESEARCH ARTICLE

Pulses of Notch activation synchronise oscillating somite cells and entrain the zebrafish segmentation clock

Cristian Soza-Ried, Emre Öztürk*, David Ish-Horowicz and Julian Lewis‡

ABSTRACT

Formation of somites, the rudiments of vertebrate body segments, is an oscillatory process governed by a gene-expression oscillator, the segmentation clock. This operates in each cell of the presomitic mesoderm (PSM), but the individual cells drift out of synchrony when Delta/Notch signalling fails, causing gross anatomical defects. We and others have suggested that this is because synchrony is maintained by pulses of Notch activation, delivered cyclically by each cell to its neighbours, that serve to adjust or reset the phase of the intracellular oscillator. This, however, has never been proved. Here, we provide direct experimental evidence, using zebrafish containing a heat-shock-driven transgene that lets us deliver artificial pulses of expression of the Notch ligand DeltaC. In DeltaC-defective embryos, in which endogenous Notch signalling fails, the artificial pulses restore synchrony, thereby rescuing somite formation. The spacing of segment boundaries produced by repetitive heat-shocking varies according to the time interval between one heat-shock and the next. The induced synchrony is manifest both morphologically and at the level of the oscillations of *her1*, a core component of the intracellular oscillator. Thus, entrainment of intracellular clocks by periodic activation of the Notch pathway is indeed the mechanism maintaining cell synchrony during somitogenesis.

KEY WORDS: Notch, Delta, Segmentation clock, Somites, Zebrafish, Oscillation

INTRODUCTION

Viewed as biochemical machines, individual cells are noisy and erratic. This is an unavoidable consequence of their small size and the stochastic nature of chemical reactions involving small numbers of molecules, and it is manifest in random variation in the levels and timing of gene expression. In spite of this cell variability, the multicellular patterns formed as an animal develops are remarkably precise. Through cell-cell communication, neighbouring cells coordinate their activities, giving rise to collective behaviour that is more accurate and predictable than that of any individual cell (Gurdon et al., 1993). The mechanisms that coordinate the behaviour of neighbours in the face of random variation thus play a key part in the production of a properly patterned body.

In this article, we focus on an aspect of development that illustrates these principles in a particularly striking way: the segmentation of the vertebrate body axis. In this process, timing is crucial, and the final spatial pattern depends on temporal coordination of oscillations in individual cells. When the cells that are destined to form the body segments fail to communicate properly and so lose coordination, the noisiness of cell behaviour makes itself manifest in a gross disorder of the adult pattern of vertebrae and associated segmental structures (Jiang et al., 2000; Pourquie, 2011). Our goal here is to understand how the coordination is achieved.

The segments derive from bilateral blocks of mesoderm called somites, which form in head-to-tail sequence in two symmetrical rows flanking the central axis of the embryo (reviewed by Gridley, 2006; Holley, 2007; Lewis et al., 2009; Oates et al., 2012; Pourquie, 2007; Stern and Vasiliauskas, 2000). A region of undifferentiated proliferative tissue at the tail end of the embryo, called the presomitic mesoderm (PSM), is the source of the new somite cells. The extent of the PSM is governed by Wnt and Fgf signals produced in the tail bud. As the PSM cells proliferate, those at the anterior end of the PSM move out of the range of action of these posterior signals and begin differentiation, breaking up into blocks (the somites) separated by clefts (the segment boundaries).

This physical segmentation is foreshadowed by a periodic pattern of gene expression in the PSM driven by a molecular oscillator, the segmentation clock, that serves to define the positions of the segment boundaries (Palmeirim et al., 1997). As cells emerge from the posterior part of the PSM, they slow down and finally halt their oscillation. In so doing, they become stamped with different gene expression identities according to their clock phase at the time of exit (to be precise, at their time of crossing a determination boundary that demarcates anterior from posterior PSM) (Giudicelli et al., 2007). Through this process, operating repetitively, one additional somite pair is created in each cycle of the segmentation clock. The length of this cycle, i.e. the period of oscillation of the cell clocks in the posterior PSM [which equals that of the spatial pattern of gene expression in the PSM as a whole (Giudicelli et al., 2007; Morelli et al., 2009)], depends on the species and the temperature; in zebrafish, it is 37 min at 23°C, 23 min at 28°C (Schroter et al., 2008).

The set of oscillatory PSM genes varies from species to species, but in all vertebrates analysed so far it includes one or more members of the Hes/Her family (Krol et al., 2011). These are direct targets of regulation by Notch, and they code for inhibitory basic helix-loop-helix (bHLH) transcription regulators. In the zebrafish, the key oscillator genes are thought to be *her1* and *her7*. These are closely linked and co-regulated, and they function quasi-redundantly. They are directly inhibited by their own protein products, and the delayed negative feedback due to this intracellular autoinhibitory loop is thought to be the fundamental generator of the oscillations of the segmentation clock (Bessho et al., 2003; Henry et al., 2002; Holley et al., 2002; Lewis, 2003; Oates and Ho, 2002; Schroter et al., 2012; Shankaran et al., 2007; Trofka et al., 2012).

Vertebrate Development and Developmental Genetics Laboratories, Cancer Research UK London Research Institute, 44 Lincoln's Inn Fields, London WC2A 3LY, UK.
*Present address: Intel Ankara Office, Bilkent Plaza Building A-3 Kat 5/No: 54, Bilkent, Ankara 06800, Turkey.

‡Author for correspondence (julian.lewis@cancer.org.uk)

Received 1 August 2013; Accepted 21 February 2014

Development (2014) 141, 1780-1788 doi:10.1242/dev.102111

When *her1* and *her7* are deleted, the clock fails (Henry et al., 2002; Oates and Ho, 2002; Oates et al., 2005). Somitic tissue is still produced according to the normal timetable, and segment boundary markers, such as *cb1045* mRNA (Riedel-Kruse et al., 2007), are eventually expressed; but instead of marking out complete regularly spaced stripes, they show up in an irregular pattern, with fragments of boundary distributed in a higgledy-piggledy fashion. The outcome in the adult is disordered segmentation all along the body axis.

When Notch signalling is blocked, either by mutations in Notch pathway components, such as the Notch ligand DeltaC (Julich et al., 2005; Mara et al., 2007; Oates et al., 2005; Wright et al., 2011), or by γ-secretase inhibitors, such as DAPT (Ozbudak and Lewis, 2008; Riedel-Kruse et al., 2007), one sees a superficially similar but subtly different phenotype: posterior segmentation is disrupted, but the first few somites still form correctly. This suggests the following simple scenario (Jiang et al., 2000): although each cell in the PSM contains a quasi-cell-autonomous oscillator (based on *her1/7*), this oscillator is noisy and oscillations of the individual cells are normally kept in synchrony only through cell-cell communication that depends on Delta-Notch signalling. When this signalling fails, the cells start out synchronous (all obedient to the same starting signal in the gastrula) but then drift out of synchrony over time.

Several groups have confirmed that Notch signalling is required for maintenance of synchrony (Horikawa et al., 2006; Mara et al., 2007; Ozbudak and Lewis, 2008; Riedel-Kruse et al., 2007); that the *her1/7* genes lie in the Notch pathway and are regulated by Notch as well as by their own products (Holley et al., 2000; Ozbudak and Lewis, 2008; Shankaran et al., 2007); that Notch signalling can modulate the period of the collective oscillation in accordance with the theory of loosely coupled oscillators (Herrgen et al., 2010; Morelli et al., 2009); that DeltaC (which oscillates, driven by *her1/7*) and DeltaD (which does not) collaborate to activate Notch cyclically (Mara et al., 2007; Wright et al., 2011); and, most recently, that in zebrafish in which Notch signalling is defective, individual PSM cells do indeed continue to show oscillating expression of *her1/7* but with random fluctuations in period, phase and amplitude (Delaune et al., 2012; Masamizu et al., 2006). All these findings can be represented in a mathematical model in which the oscillations of DeltaC provide a signal that each cell displays on its surface, informing its neighbours about its own cycle phase and entraining them all to the same rhythm by adjusting their individual clocks (Lewis, 2003) (for various subsequent formulations and modifications, see Agrawal et al., 2009; Ay et al., 2013; Baker et al., 2008; Campanelli and Gedeon, 2010; Cinquin, 2007; Feng and Navaratna, 2007; Hanisch et al., 2013; Horikawa et al., 2006; Leier et al., 2008; Momiji and Monk, 2008; Terry et al., 2011). We have measured several of the parameters of this model and have shown that it can successfully account for the phenomena (Giudicelli et al., 2007; Hanisch et al., 2013).

In spite of all this circumstantial evidence, we still have no direct proof that Notch signalling maintains synchrony in the manner proposed, through periodic pulses of Notch activation that entrain the intracellular clocks. Indeed, some data in the mouse might be taken to cast doubt on this idea: some accounts report that Delta1 (Dll1, the mammalian counterpart of DeltaC and DeltaD) does not oscillate in the mouse PSM or oscillates only weakly (Krol et al., 2011), and other findings in the mouse suggest that segmentation does not depend on cyclic variation in the level of activated Notch (NICD) (Feller et al., 2008).

In this article, we use zebrafish containing a transgene that allows us to generate, by heat-shock, artificial pulses of expression of the key Notch ligand DeltaC. In this way, we can see how pulses of Notch activation affect the segmentation clock.

RESULTS

A heat-shock-driven *deltaC* transgene allows us to trigger brief pulses of *deltaC* overexpression

To generate pulses of activation of the Notch pathway, we created transgenic fish containing a construct in which an *hsp70* heat-shock promoter drives expression of *deltaC*. The full *deltaC* 3′UTR was included with the aim that the resulting transcript should be turned over with a short lifetime similar to that of normal endogenous *deltaC* mRNA. Two independent transgenic lines were obtained and characterised by analysis of expression of *deltaC* mRNA and DeltaC protein following heat-shock. Both lines behaved similarly (not shown) and as expected, and we used just one of them, named *Tg(hsp70l:dlc)*, for subsequent experiments.

Fig. 1A shows the time course of expression of the transgene following a single 15-min heat-shock in embryos with intact normal endogenous *deltaC*. Heat-shocked transgenics were compared with two types of controls: transgenic embryos that were not heat-shocked, and wild-type heat-shocked embryos. Both controls exhibited the normal endogenous *deltaC* mRNA pattern, largely confined to the PSM region, with faint expression also in the posterior halves of formed somites. The heat-shocked transgenics, by contrast, showed ectopic expression of *deltaC* mRNA throughout the body. This was detectable within 7 min after the beginning of the heat-shock and peaked 15 min after the end of the heat-shock in all tissues. By 30 min after the end of the heat-shock, expression was still strong in the anterior half of the transgenic embryos but had declined markedly in the PSM. By 45 min after the end of the heat-shock, *deltaC* mRNA expression in the PSM, the formed somites and the posterior neural tube had fallen to wild-type levels, leaving only the normal stripy pattern of mesodermal expression of the endogenous gene. By contrast, levels of heat-shock-induced *deltaC* mRNA remained high in the brain and eyes, where there was scarcely any perceptible decline even 90 min after the end of the heat-shock. These results indicate that *deltaC* mRNA is degraded very fast in the PSM, but far more slowly in brain and eyes.

The transgenic protein appeared to be expressed in a similar way to the mRNA, as a brief pulse in the PSM (supplementary material Fig. S1) and more persistently in the brain and eyes, although the time course is complex, involving a delay for trafficking of Delta to its site of action in the plasma membrane (C.S.-R., D.I.-H. and J.L., unpublished data). The rapid turnover of *deltaC* mRNA and protein in the PSM was predicted by previous work (Giudicelli et al., 2007; Lewis, 2003) and means that our heat-shock procedure indeed gave rise to a transient pulse of DeltaC overexpression in the tissue of interest.

Repeated heat-shocks in transgenic embryos induce repeated pulses of *deltaC* expression

To check whether repeated heat-shocks would induce repeated pulses of *deltaC* mRNA expression, we subjected batches of *hsp70:deltaC* transgenic embryos to five heat-shocks separated by recovery periods of 25 min at 23°C (Fig. 1B). We fixed subsets of embryos immediately before and immediately after each pulse and measured *deltaC* mRNA expression in the PSM by quantitation of the fluorescence *in situ* hybridisation (FISH) signal, as illustrated in Fig. 1C,D.

The results (Fig. 1D) show that, although sensitivity to heat-shock becomes attenuated as the fish become acclimatised to the repeated periods at high temperature, there still is a clear response:

Development (2014) 141, 1780-1788 doi:10.1242/dev.102111

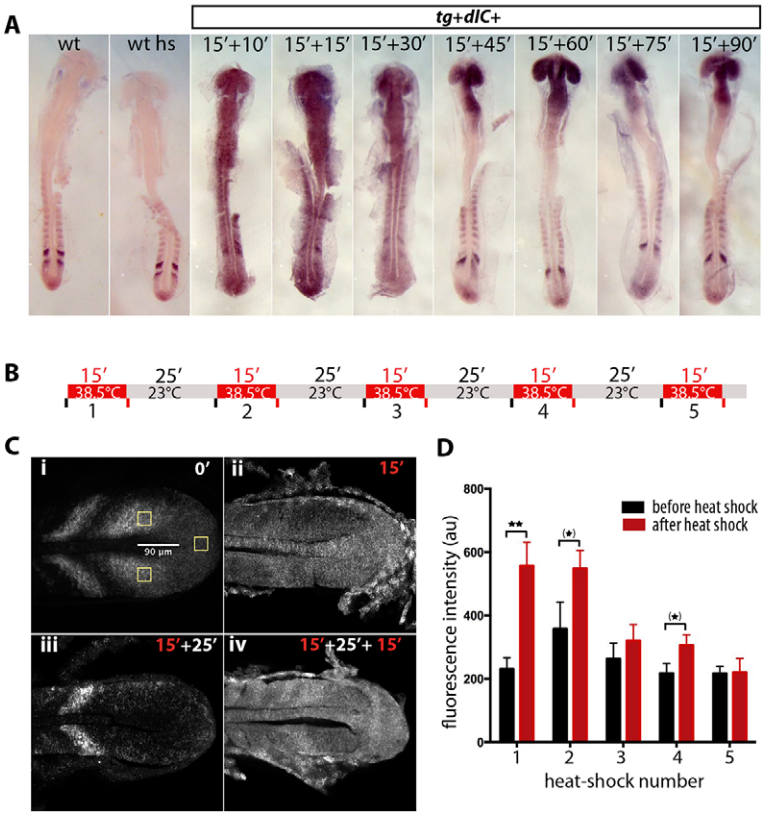

Fig. 1. Time course of *deltaC* expression in heat-shocked *Tg(hsp70l:dlc)* transgenic embryos. (A-D) Embryos at 14-16 hpf were heat-shocked at 38.5°C either once, for 15 min, with recovery at 28.5°C (A) or repeatedly (B-D), with recovery at 23°C between heat-shocks. (A) Whole mounts stained by ISH with a probe for *deltaC* mRNA, at different times after the single heat-shock, along with wild-type controls either heat-shocked (*wt hs*) or not (*wt*). $n \geq 7$ for each time point. (B) Scheme of the repetitive heat-shock treatment. (C,D) Samples were fixed for FISH with *deltaC* riboprobe before and after each heat-shock; fluorescence was measured by confocal microscopy as an average over the three boxed regions (30×30 µm^2) marked in panel Ci. (C) Specimens before and after the first (i,ii) and second (iii,iv) heat-shocks. (D) Measurements for embryos subjected to up to five heat-shocks. Values are means of *n* embryos fixed before and after the end of each heat-shock, where (n_{before}, n_{after})=(9, 10), (4, 4), (7, 4), (5, 3) and (7, 7) for the successive heat-shocks. Error bars show s.e.m. Asterisks indicate statistical significance of the difference between measurements before and after the given heat shock: *$P \leq 0.06$; **$P < 0.001$; one-tailed *t*-test.

the series of five successive heat-shocks produces at least three distinct pulses of *deltaC* expression in the PSM.

A pulse of transgenic DeltaC can cause a somite boundary shift

To see how a pulse of DeltaC would affect the pattern of segmentation, we began by delivering a single heat-shock to embryos that contained the transgene but were otherwise wild type, with the normal *deltaC* gene intact; we call these *tg+;dlc+* embryos. In the absence of heat-shock, such embryos showed a normal wild-type pattern of segmentation (Fig. 2). Heat-shocked wild-type control embryos lacking the transgene also showed normal segmentation. [In another wild-type strain of zebrafish, as in chick embryos (Primmett et al., 1988), heat-shock by itself has been reported to cause somite abnormalities (Roy et al., 1999), but this was not the case for our fish.]

Results for *tg+;dlc+* embryos following a single heat-shock (Fig. 2) were more variable, but, taken together, revealed marked effects. Although some showed a normal segmentation pattern (20/73), others showed a single somite (or somite pair) that was either larger (7/73) or smaller (12/73) than normal, followed by a series of normal somites, and still others showed one or two fragmented somite boundaries, followed again by normal somites (19/73).

These results are just as one would expect if a pulse of Notch activation can reset the phase of the segmentation clock. The effect of a single artificial pulse of DeltaC in an embryo with its own intact DeltaC-coupled oscillator will depend on the timing of the artificial pulse relative to the pulsations of the endogenous oscillator in the crucial region (the posterior PSM). If the two occur in synchrony, no disruption is expected. If they are not in synchrony, then the artificial pulse is expected to shift the phase of the endogenous oscillator, hastening or delaying the next peak and so giving a shortened or lengthened somite, after which the endogenous oscillator will be left in full control and should continue operating normally, giving subsequent somites that are normal. Lastly, if the artificial pulse clashes in an extreme way with the endogenous oscillation (e.g. if the peak of the former occurs at a trough of the latter), we may expect a disorderly result, with transient loss of synchrony between cells, leading to production of one or two fragmented somite boundaries, followed again by normal somites as the endogenous system picks up control.

A single heat-shock in a DeltaC-deficient background rescues the formation of several somites

When somitogenesis begins, oscillation of the segmentation clock genes starts synchronously in all PSM cells. However, in embryos with a block in Notch-mediated cell-cell communication, the cells gradually drift out of synchrony until eventually segmentation is disrupted. In *deltaC* loss-of-function mutants, such as *dlc*$^{tw212b/tw212b}$ (*bea* mutants), this occurs typically after formation of about six regular somite boundaries (delimiting five somites) at the anterior end of the body (Jiang et al., 2000; Julich et al., 2005; Ozbudak and Lewis, 2008; van Eeden et al., 1998) (supplementary material Fig. S2). Subsequent somite boundaries, as revealed by the myotome boundary marker *cb1045*, are fragmented and irregular (Fig. 2B and Fig. 3B; supplementary material Fig. S2).

How would such a system respond to an artificial pulse of DeltaC, delivered to all cells simultaneously? To find out, we took mutant embryos lacking functional endogenous DeltaC and containing the heat-shock-driven transgene and gave them, in a first series of experiments, a single standard 15-min heat-shock. This was delivered at 15-15.5 hours post-fertilisation (hpf), corresponding to the 12- to 13-somite stage in a normal embryo. The embryos were then left to continue development at 28.5°C until 48 hpf, when they were fixed and stained (Fig. 3D; supplementary material Fig. S3). In 21 out of

Development (2014) 141, 1780-1788 doi:10.1242/dev.102111

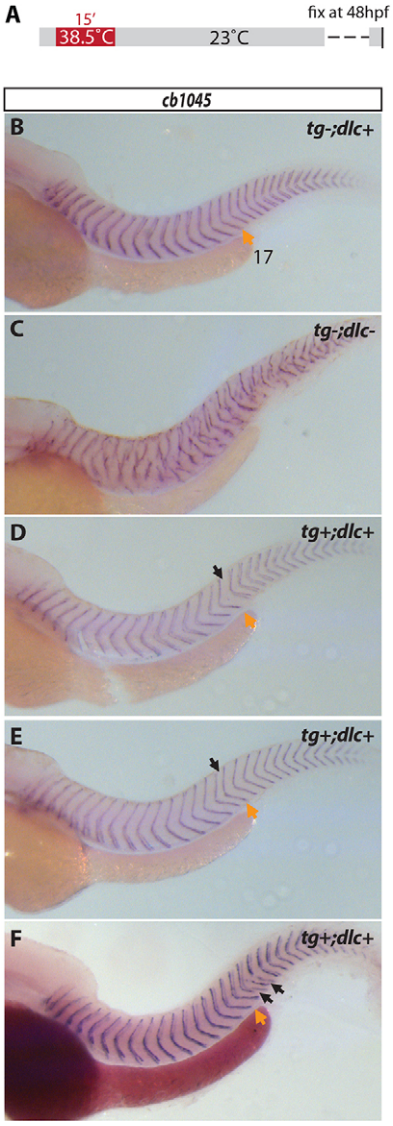

Fig. 2. *tg+;dlC+* embryos subjected to a single heat-shock, compared with the wild-type and *dlc*$^{-/-}$ non-transgenic controls. Transgenic *tg+;dlc+* embryos at the 14-somite stage were given a single 15-min heat-shock, left to develop at 28.5°C until 48 hpf, and then fixed and stained as whole mounts by ISH for the somite boundary marker *cb1045*. (A) Scheme of the heat-shock treatment. (B) Control heat-shocked wild-type embryo. (C) Control non-heat-shocked *tg−;dlc−* (*dlc*$^{tw212b/tw212b}$, *beamter*) embryo. (D-F) Heat-shocked *tg+;dlc+* embryos. Arrows indicate disrupted (F) or abnormally small (E) or large (D) segments.

21 *tg+;dlc−* embryos, at least one, and usually two to five (mean±s.e.m.=4.1±0.3, *n*=21), regularly formed and correctly spaced somite boundaries could be seen where, in the absence of heat-shock, there would have been only a fragmented and irregular pattern. The anteriormost rescued boundaries were at levels roughly corresponding to somites 15 to 19 of a normal embryo (Fig. 3D; supplementary material Fig. S3 and Fig. S4B); it is difficult to be exact, without a full series of well-formed somites as markers. This estimated location is on average three to five somite-widths posterior to the level that might have been expected if the heat-shock exerted its reorganising effect immediately in the tissue emerging from the anterior end of the PSM at the time of heat-shock.

These results indicate that the artificial pulse of DeltaC in a DeltaC-defective embryo is able to knock the desynchronised cells back into synchrony, for a while at least, to a degree sufficient for production of properly organised somite boundaries. Two questions arise, however. First, why is there a delay (the posterior shift) in the production of rescued somite boundaries? This result is to be expected because cells in the anterior half of the PSM are already determined with regard to the action of the segmentation clock on segment boundary formation (Giudicelli et al., 2007; Ozbudak and Lewis, 2008). The rescued somites should correspond to cells that were in the posterior half of the PSM at the time of the shock and so had not yet crossed the determination boundary. Second, why does the single heat-shock give several rescued somite boundaries, not just one? We suppose that this is because desynchronisation is gradual: cells that have been synchronised take several cycles to drift out of synchrony when cell-cell communication is defective, just as in the initial development of DeltaC-deficient embryos, which still produce the first few somite boundaries.

Heat-shocks repeated at an appropriate frequency give increased numbers of rescued somite boundaries

According to the above argument, we should be able to delay the loss of synchrony and obtain increased numbers of rescued somite boundaries by repeating the heat-shocks at an appropriate frequency. With a 40-min repetition time, consisting of 15 min at 38.5°C followed by 25 min at 23°C, we did indeed see this effect (Fig. 3D-G). Whereas a single heat-shock typically gave two to five rescued boundaries (see supplementary material Fig. S3 for the range of variation), multiple shocks gave additional rescued boundaries; four shocks, for example, gave a tidy series of six to eight (mean±s.e.m.=7.0±0.25; *n*=29).

With heat-shocks starting at the 3-somite stage, instead of the 13-15 somite stage, the results were similar, but with the region of rescued segmentation now located about ten somite widths more anteriorly (supplementary material Fig. S4). Thus, the first five or six boundaries, which form in a DeltaC-defective embryo even without any heat-shocking, were closely followed by a series of seven to eight normal boundaries rescued by the heat-shocks.

Repeated heat-shocks can drive the segmentation clock to depart from its natural frequency

How should we expect the system to respond to heat-shocks repeated with other frequencies, differing from the natural frequency of the segmentation clock? If the endogenous *her1/her7* oscillator in each cell is placed in conflict with an artificially imposed DeltaC oscillation, there is no reason to suppose that the latter should simply overwhelm the former, or vice versa. Rather, we should expect qualitatively different results according to the heat-shock frequency (and strength) (Strogatz, 1994). Thus, a small discrepancy in the periods might be expected to give rescue of collective oscillation but with a slightly altered period, whereas a large discrepancy (by a non-integral number of clock cycles) might lead to a breakdown of collective oscillation or to irregular or grossly abnormal oscillation cycles, such as strong peaks alternating with weak peaks. A heat-shock repetition period that was twice as long as the natural oscillation period (or *n* times as long, with *n* an integer), however, might be expected to give a prolonged rescue of collective oscillation with the normal periodicity, by acting in every second (or *n*th) clock cycle to reinforce synchrony. Effects on the oscillation period would be expected to show up in the pattern of somites, because the size of a somite is proportional to the amount of tissue exiting the PSM in one clock cycle.

To explore the behaviour experimentally, we exposed *tg+;dlc−* embryos to four heat-shocks repeated at various different

Development (2014) 141, 1780-1788 doi:10.1242/dev.102111

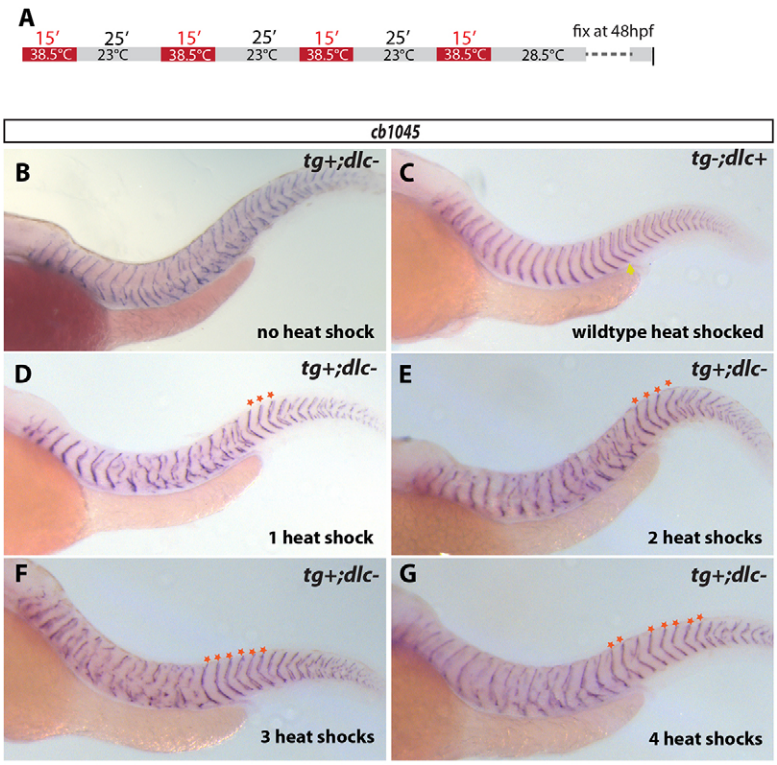

Fig. 3. Rescue of segmentation by artificial pulses of *deltaC* expression in *dlctw212b/tw212b* embryos. Transgenic *tg+;dlc–* embryos (lacking endogenous functional DeltaC) at the 11-12 somite stage were heat-shocked one, two, three or four times, or not at all, left to develop at 28.5°C until 48 hpf, and stained as in Fig. 2. Recovery periods between heat-shocks were 25 min at 23°C. (A) Scheme of the repetitive heat-shock treatments. (B-G) Typical results for each number of heat-shocks. Orange asterisks mark rescued somite boundaries. Yellow arrowhead in C marks the 17th somite boundary. Note that multiple heat-shocks increase the number of rescued somites: a single heat-shock produced 4.1±0.3 (mean±s.e.m.), two heat-shocks produced 4.7±0.4, three heat-shocks produced 5.0±0.3 and four heat-shocks produced 7.0±0.25. A wild-type (*tg–;dlc+*) embryo subjected to a series of four heat-shocks is included as a control; it shows normal segmentation (C). Each photo is representative of *n* embryos examined, where *n*=8 for the heat-shocked wild type, and *n*=20, 21, 22, 22 and 29 for the *tg+;dlc–* embryos subjected to zero, one, two, three and four heat-shocks, respectively.

intervals. Fig. 4 and supplementary material Fig. S5 show representative results. Rescue seemed to be best (in terms of the normality of the rescued somites) for periodicities of 15+25 min (as described above) and 15+30 min. The 15+15 and 15+20 min series, with the shortest periodicity, showed a slightly less extensive rescue and in a few cases somites that were distinctly smaller than normal, whereas the 15+35 min series showed occasional somites that were distinctly bigger. Still longer periods (15+40, 15+45, 15+50 and 15 +60 min) still gave some rescue, but with more irregularities and more frequent abnormally large somites in the region of rescue (Fig. 4D-E′). These enlarged somites often had a fragmentary somite boundary midway between their two well-marked boundaries, suggesting an alternation of strong and weak peaks of the segmentation clock oscillation, with weak peaks translating into only a fragment of boundary (Fig. 4D-E′, arrowheads). Strikingly, a heat-shock period of 15+65 min, which we estimate to be close to twice the natural fundamental clock period (i.e. the period in the posterior PSM) for the given temperature regime, gave an extended series of well-formed somites that were only slightly larger than normal (Fig. 4F,F′).

We measured the spacing between somite boundaries for at least eight embryos for each heat-shock treatment pattern, focusing on the region spanning somites six to nine inclusive, corresponding to cells that had crossed the determination front during the period of repetitive heat-shocking and thus were expected to display its effect most directly. As shown in Fig. 4G, there is a clear trend towards increased width of the rescued somites with increasing time between heat-shocks, but with a reversion to near normal size with the 15+65 min regime. These results are consistent with the predictions described above and show that it is possible to force the segmentation clock to oscillate with an altered period by modifying the timing of repeated pulses of Notch pathway activation.

Note, however, that we should not expect, and do not see, a precise (linear) proportionality between somite size and the pulse repeat period, even for moderate values of that period. First, heat-shock responses are variable and not every one is guaranteed to be effective (Fig. 1; supplementary material Fig. S3). Second, somite length may be constrained to some extent by other factors in addition to the segmentation clock machinery, such as cell-biological constraints on the length of the myotome (muscle) cells, each of which has to span precisely the distance from one somite boundary to the next. Lastly, according to standard clock-and-wavefront theory, the size of a somite is proportional to the amount of tissue exiting the PSM in one clock cycle, and thus depends not only the (forced) period of the cycle but also on the length of the PSM and the growth rate (cell population doublings per unit time) in the PSM. The PSM growth rate and length might themselves be affected by the heat-shocks.

In fact, in normal embryos, both the clock rate and the growth rate (but not the length of the PSM) are strongly temperature dependent and vary in parallel in such a way that somite size (which depends on their ratio) is kept practically constant (Schroter et al., 2008). Repetitive heat-shocking, therefore, might be expected to raise the growth rate (and to do so the more strongly, the shorter the intervals between shocks), while at the same time holding the clock period locked to the heat-shock repetition period. In its effect on somite size, the accelerated growth rate would tend to compensate for an accelerated repetition rate, but to exaggerate the consequences of a decreased repetition rate. This could explain the observation (Fig. 4) that artificial pulsing at a rapid rate leaves somite size relatively unaffected, whereas pulsing at a slow rate gives rise to large somites.

To check for the further possibility that the heat-shock treatment might alter the size of the PSM, we fixed a subset of embryos immediately after the end of a series of heat-shocks separated by recovery periods at 23°C, and stained them by *in situ* hybridisation (ISH) for *mespb* and *deltaC* mRNA, as markers of the anterior boundary of the PSM (Nomura-Kitabayashi et al., 2002; Sawada et al., 2000). In a first set of embryos, we used three heat-shocks separated by 25-min recovery periods; in a second set, we used four heat-shocks separated by 65-min recovery periods. As shown in

Development (2014) 141, 1780-1788 doi:10.1242/dev.102111

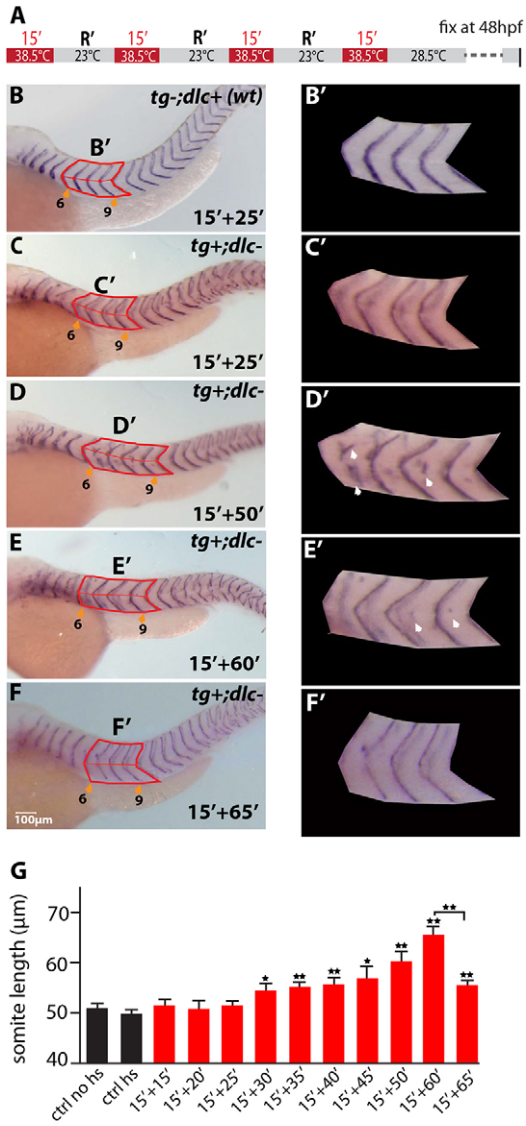

Fig. 4. Somite widths can be modified by varying the interval between heat-shocks. Batches of *tg+;dlc−* embryos were taken at the 3-somite stage and heat-shocked four times as in Fig. 3, but with different recovery times, R, between one heat-shock and the next for the different batches. (A) Scheme of heat-shock treatment. (B-F) Typical results for different heat-shock repetition cycle times, from 15+15 min (i.e. 15 min at 38.5°C followed by 15 min at 23°C) to 15+65 min. (B) A control (*tg−;dlc+*) wild-type embryo heat-shocked four times on a 15+25 min schedule. (C-F) *tg+;dlc−* embryos subjected to various different heat-shock regimes as indicated. Repetitive heat-shock rescued somite boundary formation to a sufficient extent in almost every case to allow measurement of somite width. (B′-F′) Detailed views of the region measured for each batch, corresponding to the sixth to the ninth somite (red boxes in B-F). White arrowheads in D′ mark fragments of somite boundary in the middle of giant somites. (G) Histogram of mean somite width (defined as distance from the vertex of one somite-boundary chevron to the next, shown by red line in B-F) for the measured region, as a function of heat-shock repetition cycle time. Note that embryos with heat-shock repetition cycle times of 15+30 min to 15+60 min produce bigger somites than those observed in the non-heat shocked controls (ctrl no hs) in the evaluated region, with reversion to a size only slightly greater than control at 15+65 min. **P*<0.05; ***P*<0.005, two-tailed *t*-test.

supplementary material Fig. S6, we found no significant difference in PSM length when we compared *tg+;dlc−* embryos treated in either of these ways with wild-type control embryos treated in the same way.

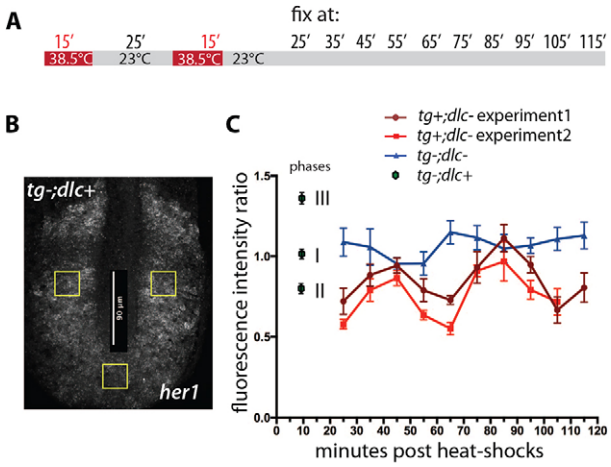

Fig. 5. Rescued somite boundary formation correlates with rescued coordination of *her1* oscillation. Mutant *tg+;dlc−* embryos were taken at the 12-somite stage, given two standard 38.5°C heat-shocks separated by 25 min at 23°C, and then maintained at 23°C for varying lengths of time before fixation. (A) Scheme of the treatment. (B) Wild-type embryo stained by FISH with *her1* riboprobe, indicating the regions chosen for measurement (30×30 µm^2 yellow boxes) for all specimens in this experiment. Scale bar (vertical): 90 µm. Fluorescence intensity was measured photometrically from *z*-stack projections. As an indicator of coordinated *her1* oscillation, we took the ratio of the level of *her1* in the extreme posterior box to the levels in the two symmetrically placed more anterior (mid-PSM) boxes. (C) Graph of this ratio as a function of time after the end of the second heat-shock. Two repetitions of the whole experiment are shown (brown and red lines), along with corresponding measurements for control *tg−;dlc−* embryos (blue line). Each data point is an average over at least three, and on average 5.4, specimens; error bars show s.e.m. Both repetitions of the heat-shock experiment show similar clear oscillations, with period of ~40 min, as expected for the segmentation clock at 23°C (Schroter et al., 2008). By contrast, the control series of *deltaC*$^{-/-}$ embryos without heat-shock shows only small fluctuations. The measurements for control *tg−;dlc+* embryos are at the left-hand side of the plot, and assigned to cycling phase I, II or III [nomenclature of Pourquie and Tam (Pourquie and am, 2001)].

Rescued somite boundary formation correlates with rescued coordination of *her1* oscillation

If our theories are correct, rescue of segmentation should depend on rescued coordination of the segmentation clock. That is, the *her1* oscillators in the individual PSM cells, which are desynchronised in the *deltaC*$^{-/-}$ loss-of-function mutant, should be driven back into synchrony by the heat-shock-driven pulses of DeltaC. Following this re-setting by heat-shock, groups of neighbouring cells, now synchronised but released from the influence of exogenous DeltaC, should show coordinated oscillations with the amplitude and frequency appropriate to their location in the PSM. To test this prediction, we subjected the mutant *tg+;dlc−* embryos to two standard heat-shocks spaced 25 min apart, and made measurements of *her1* expression at successive times thereafter. To minimise confusion arising from random variability in the general level of *her1* FISH staining, we focused on the ratio of *her1* FISH staining intensity in the posteriormost PSM to its intensity more anteriorly, in the middle part of the PSM (Fig. 5B), where *her1* oscillations are normally most pronounced. The ratio should be the same whether the embryo is heavily stained or lightly stained, so long as the pattern of clock phases is the same. In a normal wild-type embryo, this ratio goes up and down according to the phase of the segmentation clock cycle [see, for example, Oates et al. (Oates et al., 2005) and wild-type points in Fig. 5C]. As shown in Fig. 5C, the same is true for the heat-shocked *tg+;dlc−* embryos. By contrast, *tg−;dlc−* embryos showed only weak

Development (2014) 141, 1780-1788 doi:10.1242/dev.102111

random fluctuations that were not statistically significant. We conclude that the rescue of segmentation by artificial pulses of DeltaC is indeed based on a rescue of coordinated collective oscillation of *her1* (and presumably of *her7* also).

DISCUSSION

To understand all these results and judge whether they fit expectations, an analogy is useful. The cells in the *deltaC*$^{-/-}$ PSM, with their individual *her1/7* oscillations, can be compared to a group of children on swings in a playground, swinging independently. The period of swinging will be almost the same for all of them, because the swings have the same length, but will not be exactly the same, because the children differ in their centre of gravity and in the effort they put into swinging. If they all start off swinging synchronously, they will drift out of synchrony after a few cycles. Suppose that we now give them all a similar push at the same time, corresponding to a heat-shock-driven pulse of Delta-Notch signalling. This will bring them into partial synchrony, which will persist for few cycles until they drift out of synchrony again. A series of pushes delivered with a frequency matching the natural pendulum frequency of the swings will sustain synchrony for a larger number of cycles. Pushes repeated with a periodicity that differs slightly from the natural pendulum frequency will force swinging with a slightly altered period. Pushing with a frequency that clashes more seriously with the natural pendulum frequency may have unpredictable or chaotic consequences. But pushing with a periodicity that is an integral multiple of the pendulum period, e.g. a push delivered in every second cycle, will maintain synchronised swinging at the pendulum frequency.

For a more formal assessment of the implications of our experimental findings, we make comparison with the predictions of a mathematical model developed previously (Hanisch et al., 2013; Lewis, 2003). This model describes how the oscillations of the segmentation clock are generated and how Delta/Notch signalling acts to keep the individual PSM cells synchronised. The essentials of the gene control circuitry are shown in Fig. 6. The basic ideas are as follows.

(1) The mechanism of oscillation. In each cell, the protein products of the *her1* and *her7* genes exert a direct negative-feedback control of the expression of *her1* and *her7*. This gives rise to oscillatory expression of the genes with a period that is determined by the delay in the negative-feedback loop.

(2) The source of noise. Although many factors may contribute to noise and random irregularity of cell behaviour, including effects of passage through the cell cycle (Delaune et al., 2012; Horikawa et al., 2006), our model focuses on just one fundamental source of noise that is necessarily present and is quantifiable (Lewis, 2003) (R. Jenkins, A. Hanisch, C.S.-R. and J.L., unpublished): the stochastic nature of the association-dissociation reaction between the Her1 and Her7 protein complexes and the regulatory DNA that they bind to. When the cells are uncoupled, the result is that each oscillates independently with a period and amplitude that vary somewhat from cell to cell and from cycle to cycle. The magnitude of this random variation is governed by the laws of chemical kinetics and is determined by the mean lifetime of the bound state, i.e. the mean time one must wait for the inhibitory protein complex to dissociate from its DNA binding site. This waiting time is variable in the same way as the timing of a radioactive decay.

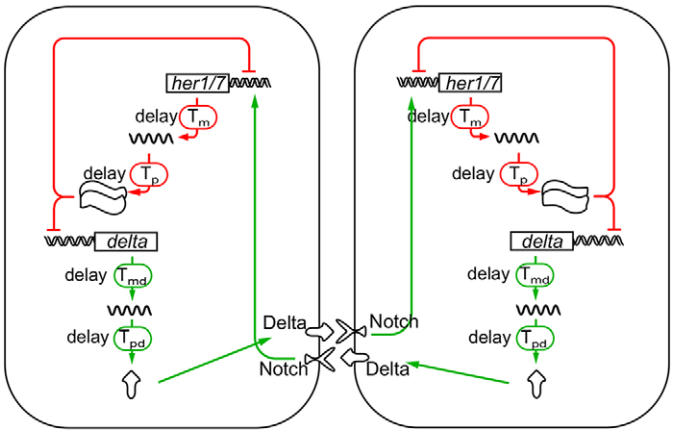

Fig. 6. The postulated gene control circuitry of the segmentation clock, shown for a representative pair of adjacent cells. Reproduced from Lewis (Lewis, 2003), with kind permission from Cell Press.

(3) The coupling between cells. In a genetically normal animal, adjacent cells are coupled through the Notch pathway. Her1/7 protein controls not only its own production, but also that of DeltaC, levels of which consequently oscillate in each cell. High levels of DeltaC activate Notch in the adjacent cell, and the activated Notch (the cleaved intracellular domain, NICD) enters the nucleus and modulates the expression of *her1/7*, giving in effect a 'push' to the intracellular oscillator. Specifically, our model supposes that NICD competes with Her1/7 protein for binding to the *her1/7* regulatory DNA: a pulse of NICD activates *her1/7* transcription by preventing Her1/7 from binding and exerting inhibition (Ozbudak and Lewis, 2008).

The 'push' exerted by a pulse of NICD may advance or retard the oscillation phase of the neighbouring cell relative to that of the DeltaC-expressing cell, depending on the delay in the signalling pathway. Numerical experimentation with our computer model, as well as sophisticated mathematical analysis of the general theory of weakly coupled oscillators (Herrgen et al., 2010; Morelli et al., 2009), confirms that such a mechanism can work to maintain synchrony across a broad expanse of PSM cells, using only an interaction between nearest neighbours.

Supplementary material Fig. S7 shows the results of computer simulations of our heat-shock experiments, using the model outlined above and developed by Hanisch et al. (Hanisch et al., 2013): for full details and an explanation of the mathematical model, representing a system of arbitrarily many coupled noisy Her1/7 oscillators, see supplementary material files M1 and M2 (M1 is an executable Mathematica notebook; M2 is the same thing as a straightforwardly readable pdf). The model shows the same behaviours that we observed experimentally. Thus, in the model, a single shock to the wild-type system causes either no abnormality or abnormality of a single somitogenesis cycle, according to the phasing of the shock (supplementary material Fig. S7A,B). A single shock in a *deltaC*$^{-/-}$ system forces the cells back into synchrony, which persists for a few cycles until they once again drift out of synchrony (supplementary material Fig. S7C). A repetitive series of shocks at the natural frequency gives additional cycles of coordinated oscillation at that frequency (supplementary material Fig. S7D). Repetitive shocks with a different repetition period can give coordinated oscillations with an altered period (supplementary material Fig. S7E,F); for example, a series of four shocks with a repetition cycle much longer than the natural clock cycle (by a non-integral factor) gives a series of four prolonged segmentation clock cycles of abnormal shape, corresponding to enlarged somites with a blip in the middle of each (supplementary material Fig. S7F). All these model predictions echo our experimental findings, which thus corroborate the original theory: periodic activation of the Notch pathway is the mechanism maintaining synchrony between cells in the segmentation clock.

Development (2014) 141, 1780-1788 doi:10.1242/dev.102111

The gene regulatory circuitry of Notch signalling in our model of the PSM is essentially the same as that mediating lateral inhibition in other systems, but the outcome is radically different (Lewis et al., 2009). Instead of generating a pepper-and-salt mixture of cells in opposite states, Notch signalling here keeps cells in unison. This is because of the powerful effect of the Her1/7 delayed negative-feedback loop, which drives the cells to oscillate individually and leads to completely different collective behaviour when the cells are coupled via the Notch pathway. Such phenomena are hard to explain through informal intuitive reasoning: to understand and predict them, mathematical modelling is essential.

Taken together with previous loss-of-function experiments, our findings are compelling evidence that pulsatile Notch signalling is the necessary and sufficient mechanism for maintenance of cell synchrony in the segmentation clock, and we have shown that pulses of Notch activation achieve this by re-setting the phases of the intracellular oscillators. Our analysis of Notch signalling in the zebrafish segmentation clock may be a useful paradigm for exploration of the mechanisms and consequences of synchronisation in other systems of oscillatory cells.

MATERIALS AND METHODS

Ethics statement

All experiments were conducted in accordance with UK Home Office Project Licenses held by J.L. and D.I.-H.

Husbandry

Zebrafish were raised routinely at 28.5°C on a 14/10 h light/dark cycle (Kimmel et al., 1995), except for periods at other temperatures during heat-shock experiments, as described below. The genetic background for our experiments was a London outbred stock as in Collins et al. (Collins et al., 2010). Fish were staged according to Kimmel et al. (Kimmel et al., 1995).

Mutants

deltaC loss-of-function (*bea*) mutants were maintained as a homozygous viable $dlc^{tw212b/tw212b}$ stock. These fish have a cysteine-to-serine missense mutation in the seventh EGF repeat of DeltaC and are easily identified by their abnormal morphology (Julich et al., 2005). Heterozygotes are phenotypically normal.

Transgenesis

The *hsp70:dlc* transgene was created by inserting into a *pBS2* vector the full-length *deltaC* cDNA (2085 bp starting at the initial ATG) including the complete 3′UTR (1327 bp) and an SV40 polyadenylation signal sequence, under the control of the zebrafish *hsp70I* heat-shock promoter (1.5 kb). As in Wright et al. (Wright et al., 2011), the *deltaC* cDNA coding sequence retained the seventh intron but all other introns were spliced out. I-*Sce*I sites flanked this gene construct. The linearised plasmid was co-injected into fertilised eggs with I-*Sce*I meganuclease, as in Giudicelli et al. (Giudicelli et al., 2007). Living fish containing the transgene were identified from fin or tail clips by PCR (forward primer 5′-AGATTGTTCTATGTCTTTTCCTTTCC-3′, matching the final part of the 3′UTR, from nt 3790 to nt 3815; reverse primer 5′-TGGTTTGTCCAAACTCATCAA-3′, matching the sequence of the I-*Sce*I pBS2 vector). Fixed specimens containing the transgene were identified by PCR or, following heat-shock, by ISH with a *deltaC* riboprobe and/or immunostaining with zdc2 monoclonal antibody (Wright et al., 2011).

Heterozygous *hsp70:dlC* transgenic fish were crossed with $dlc^{tw212b/tw212b}$ homozygotes to give double heterozygotes, which were then crossed with $dlc^{tw212b/tw212b}$ homozygotes to obtain fish heterozygous for the transgene *hsp70:dlc* and homozygous for the *deltaC* loss-of-function mutation dlc^{tw212b}.

Heat-shock

Embryos were heat-shocked at 38.5°C for 15 min: for this, they were kept in system water in the same 50 ml flask as before the heat-shock; all but 1 or 2 ml of the water was removed from the flask and replaced with system water (20 ml) at 38.5°C, and the flask was then immediately placed in a water bath at 38.5°C. [Zebrafish in the wild can live and breed at temperatures as high 38.6°C (Engeszer et al., 2007).] In intervals between one heat-shock and the next, embryos were allowed to recover and continue development at 23°C. In our hands, wild-type embryos subjected to a succession of 38.5°C heat-shocks and 23°C recovery periods showed normal segmentation, indicating that the segmentation clock continued to operate in a properly coordinated way. To follow outcomes after the end of a series of heat-shocks, we brought embryos back to 28.5°C. Embryos were fixed in phosphate-buffered 4% paraformaldehyde.

In situ hybridisation

Whole-mount RNA *in situ* hybridisation (ISH) was performed according to standard protocols using 5-bromo-4-chloro-3-indolyl-phosphate in conjunction with nitro blue tetrazolium (NBT/BCIP) as in Schorpp et al. (Schorpp et al., 2006) and with the following digoxigenin-labelled riboprobes: *cb1045* (Riedel-Kruse et al., 2007), *deltaC* (Smithers et al., 2000) and *her1* (Takke and Campos-Ortega, 1999). For dual whole-mount RNA fluorescence *in situ* hybridisation (FISH), fluorescein-labelled *deltaC* and digoxigenin-labelled *her1* riboprobes were used and were detected, respectively, with sheep peroxidase-conjugated anti-fluorescein antibody (PerkinElmer, 1/100) and mouse peroxidase-conjugated anti-digoxigenin antibody (Jackson ImmunoResearch Laboratories, 1/1000). Peroxidase activity was assessed using tyramide signal amplification (TSA) Cyanine 3 and Cyanine 5 (PerkinElmer). Fluorescently stained specimens were counterstained with DAPI and mounted in SlowFade Gold (Invitrogen). For ISH, control heat-shocked wild-type embryos (*tg−;dlC+*) were processed in a single batch together with *tg+;dlC−*, *tg+;dlC+* and *tg−;dlC−* embryos. After photography, all embryos were genotyped by PCR.

Microscopy and imaging

For analysis of somite segmentation patterns, whole embryos were stained by NBT/BCIP ISH with *cb1045*, viewed in 70% glycerol with a Leica MZ16 stereomicroscope, and photographed with a Leica DC500 digital camera using FireCam software. Saved images were linearly adjusted in Photoshop for contrast, brightness and colour balance, taking care that any such adjustment was applied similarly (or not at all) to all specimens in any series where comparative measurements were to be made.

Fluorescently stained and immunostained specimens were flat-mounted and viewed in a Zeiss LSM700 confocal microscope with 25×/0.8 and 40×/1.2 water-immersion objectives. ImageJ software was used to measure fluorescence intensity from projections of matched sets of optical sections (*z*-stacks) in each specimen.

Acknowledgements

We thank our aquarium staff for excellent fish care; and Caroline Hill and Maxine Holder for valuable comments on the manuscript.

Competing interests

The authors declare no competing financial interests.

Author contributions

C.S.-R., D.I.-H. and J.L. planned the experiments and wrote the paper. C.S.-R. and E.O. performed the experiments. J.L. performed the mathematical modelling.

Funding

This work was funded by Cancer Research UK.

Supplementary material

Supplementary material available online at
http://dev.biologists.org/lookup/suppl/doi:10.1242/dev.102111/-/DC1

References

Agrawal, S., Archer, C. and Schaffer, D. V. (2009). Computational models of the Notch network elucidate mechanisms of context-dependent signaling. *PLoS Comput. Biol.* **5**, e1000390.

Ay, A., Knierer, S., Sperlea, A., Holland, J. and Ozbudak, E. M. (2013). Short-lived Her proteins drive robust synchronized oscillations in the zebrafish segmentation clock. *Development* **140**, 3244-3253.

Baker, R. E., Schnell, S. and Maini, P. K. (2008). Mathematical models for somite formation. *Curr. Top. Dev. Biol.* **81**, 183-203.

Bessho, Y., Hirata, H., Masamizu, Y. and Kageyama, R. (2003). Periodic repression by the bHLH factor Hes7 is an essential mechanism for the somite segmentation clock. *Genes Dev.* **17**, 1451-1456.
Campanelli, M. and Gedeon, T. (2010). Somitogenesis clock-wave initiation requires differential decay and multiple binding sites for clock protein. *PLoS Comput. Biol.* **6**, e1000728.
Cinquin, O. (2007). Repressor dimerization in the zebrafish somitogenesis clock. *PLoS Comput. Biol.* **3**, e32.
Collins, R. T., Linker, C. and Lewis, J. (2010). MAZe: a tool for mosaic analysis of gene function in zebrafish. *Nat. Methods* **7**, 219-223.
Delaune, E. A., François, P., Shih, N. P. and Amacher, S. L. (2012). Single-cell-resolution imaging of the impact of Notch signaling and mitosis on segmentation clock dynamics. *Dev. Cell* **23**, 995-1005.
van Eeden, F. J., Holley, S. A., Haffter, P. and Nüsslein-Volhard, C. (1998). Zebrafish segmentation and pair-rule patterning. *Dev. Genet.* **23**, 65-76.
Engeszer, R. E., Patterson, L. B., Rao, A. A. and Parichy, D. M. (2007). Zebrafish in the wild: a review of natural history and new notes from the field. *Zebrafish* **4**, 21-40.
Feller, J., Schneider, A., Schuster-Gossler, K. and Gossler, A. (2008). Noncyclic Notch activity in the presomitic mesoderm demonstrates uncoupling of somite compartmentalization and boundary formation. *Genes Dev.* **22**, 2166-2171.
Feng, P. and Navaratna, M. (2007). Modelling periodic oscillations during somitogenesis. *Math. Biosci. Eng.* **4**, 661-673.
Giudicelli, F., Ozbudak, E. M., Wright, G. J. and Lewis, J. (2007). Setting the tempo in development: an investigation of the zebrafish somite clock mechanism. *PLoS Biol.* **5**, e150.
Gridley, T. (2006). The long and short of it: somite formation in mice. *Dev. Dyn.* **235**, 2330-2336.
Gurdon, J. B., Lemaire, P. and Kato, K. (1993). Community effects and related phenomena in development. *Cell* **75**, 831-834.
Hanisch, A., Holder, M. V., Choorapoikayil, S., Gajewski, M., Ozbudak, E. M. and Lewis, J. (2013). The elongation rate of RNA polymerase II in zebrafish and its significance in the somite segmentation clock. *Development* **140**, 444-453.
Henry, C. A., Urban, M. K., Dill, K. K., Merlie, J. P., Page, M. F., Kimmel, C. B. and Amacher, S. L. (2002). Two linked hairy/Enhancer of split-related zebrafish genes, her1 and her7, function together to refine alternating somite boundaries. *Development* **129**, 3693-3704.
Herrgen, L., Ares, S., Morelli, L. G., Schröter, C., Jülicher, F. and Oates, A. C. (2010). Intercellular coupling regulates the period of the segmentation clock. *Curr. Biol.* **20**, 1244-1253.
Holley, S. A. (2007). The genetics and embryology of zebrafish metamerism. *Dev. Dyn.* **236**, 1422-1449.
Holley, S. A., Geisler, R. and Nusslein-Volhard, C. (2000). Control of her1 expression during zebrafish somitogenesis by a delta-dependent oscillator and an independent wave-front activity. *Genes Dev.* **14**, 1678-1690.
Holley, S. A., Julich, D., Rauch, G. J., Geisler, R. and Nusslein-Volhard, C. (2002). her1 and the notch pathway function within the oscillator mechanism that regulates zebrafish somitogenesis. *Development* **129**, 1175-1183.
Horikawa, K., Ishimatsu, K., Yoshimoto, E., Kondo, S. and Takeda, H. (2006). Noise-resistant and synchronized oscillation of the segmentation clock. *Nature* **441**, 719-723.
Jiang, Y.-J., Aerne, B. L., Smithers, L., Haddon, C., Ish-Horowicz, D. and Lewis, J. (2000). Notch signalling and the synchronization of the somite segmentation clock. *Nature* **408**, 475-479.
Jülich, D., Hwee Lim, C., Round, J., Nicolaije, C., Schroeder, J., Davies, A., Geisler, R., Lewis, J., Jiang, Y.-J. and Holley, S. A. (2005). beamter/deltaC and the role of Notch ligands in the zebrafish somite segmentation, hindbrain neurogenesis and hypochord differentiation. *Dev. Biol.* **286**, 391-404.
Kimmel, C. B., Ballard, W. W., Kimmel, S. R., Ullmann, B. and Schilling, T. F. (1995). Stages of embryonic development of the zebrafish. *Dev. Dyn.* **203**, 253-310.
Krol, A. J., Roellig, D., Dequeant, M.-L., Tassy, O., Glynn, E., Hattem, G., Mushegian, A., Oates, A. C. and Pourquie, O. (2011). Evolutionary plasticity of segmentation clock networks. *Development* **138**, 2783-2792.
Leier, A., Marquez-Lago, T. T. and Burrage, K. (2008). Generalized binomial tau-leap method for biochemical kinetics incorporating both delay and intrinsic noise. *J. Chem. Phys.* **128**, 205107.
Lewis, J. (2003). Autoinhibition with transcriptional delay: a simple mechanism for the zebrafish somitogenesis oscillator. *Curr. Biol.* **13**, 1398-1408.
Lewis, J., Hanisch, A. and Holder, M. (2009). Notch signaling, the segmentation clock, and the patterning of vertebrate somites. *J. Biol.* **8**, 44.
Mara, A., Schroeder, J., Chalouni, C. and Holley, S. A. (2007). Priming, initiation and synchronization of the segmentation clock by deltaD and deltaC. *Nat. Cell Biol.* **9**, 523-530.
Masamizu, Y., Ohtsuka, T., Takashima, Y., Nagahara, H., Takenaka, Y., Yoshikawa, K., Okamura, H. and Kageyama, R. (2006). Real-time imaging of the somite segmentation clock: revelation of unstable oscillators in the individual presomitic mesoderm cells. *Proc. Natl. Acad. Sci. U.S.A.* **103**, 1313-1318.
Momiji, H. and Monk, N. A. M. (2008). Dissecting the dynamics of the Hes1 genetic oscillator. *J. Theor. Biol.* **254**, 784-798.
Morelli, L. G., Ares, S., Herrgen, L., Schröter, C., Jülicher, F. and Oates, A. C. (2009). Delayed coupling theory of vertebrate segmentation. *HFSP J.* **3**, 55-66.
Nomura-Kitabayashi, A., Takahashi, Y., Kitajima, S., Inoue, T., Takeda, H. and Saga, Y. (2002). Hypomorphic Mesp allele distinguishes establishment of rostrocaudal polarity and segment border formation in somitogenesis. *Development* **129**, 2473-2481.
Oates, A. C. and Ho, R. K. (2002). Hairy/E(spl)-related (Her) genes are central components of the segmentation oscillator and display redundancy with the Delta/Notch signaling pathway in the formation of anterior segmental boundaries in the zebrafish. *Development* **129**, 2929-2946.
Oates, A. C., Mueller, C. and Ho, R. K. (2005). Cooperative function of deltaC and her7 in anterior segment formation. *Dev. Biol.* **280**, 133-149.
Oates, A. C., Morelli, L. G. and Ares, S. (2012). Patterning embryos with oscillations: structure, function and dynamics of the vertebrate segmentation clock. *Development* **139**, 625-639.
Özbudak, E. M. and Lewis, J. (2008). Notch signalling synchronizes the zebrafish segmentation clock but is not needed to create somite boundaries. *PLoS Genet.* **4**, e15.
Palmeirim, I., Henrique, D., Ish-Horowicz, D. and Pourquie, O. (1997). Avian hairy gene expression identifies a molecular clock linked to vertebrate segmentation and somitogenesis. *Cell* **91**, 639-648.
Pourquie, O. (2007). Building the spine: the vertebrate segmentation clock. *Cold Spring Harb. Symp. Quant. Biol.* **72**, 445-449.
Pourquie, O. (2011). Vertebrate segmentation: from cyclic gene networks to scoliosis. *Cell* **145**, 650-663.
Pourquie, O. and Tam, P. P. L. (2001). A nomenclature for prospective somites and phases of cyclic gene expression in the presomitic mesoderm. *Dev. Cell* **1**, 619-620.
Primmett, D. R., Stern, C. D. and Keynes, R. J. (1988). Heat shock causes repeated segmental anomalies in the chick embryo. *Development* **104**, 331-339.
Riedel-Kruse, I. H., Muller, C. and Oates, A. C. (2007). Synchrony dynamics during initiation, failure, and rescue of the segmentation clock. *Science* **317**, 1911-1915.
Roy, M. N., Prince, V. E. and Ho, R. K. (1999). Heat shock produces periodic somitic disturbances in the zebrafish embryo. *Mech. Dev.* **85**, 27-34.
Sawada, A., Fritz, A., Jiang, Y.-J., Yamamoto, A., Yamasu, K., Kuroiwa, A., Saga, Y. and Takeda, H. (2000). Zebrafish *mesp* family genes, *mesp-a* and *mesp-b* are segmentally expressed in the presomitic mesoderm, and *mesp-b* confers the anterior identity to the developing somites. *Development* **127**, 1691-1702.
Schorpp, M., Bialecki, M., Diekhoff, D., Walderich, B., Odenthal, J., Maischein, H. M., Zapata, A. G. and Boehm, T. (2006). Conserved functions of Ikaros in vertebrate lymphocyte development: genetic evidence for distinct larval and adult phases of T cell development and two lineages of B cells in zebrafish. *J. Immunol.* **177**, 2463-2476.
Schröter, C., Herrgen, L., Cardona, A., Brouhard, G. J., Feldman, B. and Oates, A. C. (2008). Dynamics of zebrafish somitogenesis. *Dev. Dyn.* **237**, 545-553.
Schröter, C., Ares, S., Morelli, L. G., Isakova, A., Hens, K., Soroldoni, D., Gajewski, M., Jülicher, F., Maerkl, S. J., Deplancke, B. et al. (2012). Topology and dynamics of the zebrafish segmentation clock core circuit. *PLoS Biol.* **10**, e1001364.
Shankaran, S. S., Sieger, D., Schröter, C., Czepe, C., Pauly, M.-C., Laplante, M. A., Becker, T. S., Oates, A. C. and Gajewski, M. (2007). Completing the set of h/E(spl) cyclic genes in zebrafish: her12 and her15 reveal novel modes of expression and contribute to the segmentation clock. *Dev. Biol.* **304**, 615-632.
Smithers, L., Haddon, C., Jiang, Y.-J. and Lewis, J. (2000). Sequence and embryonic expression of *deltaC* in the zebrafish. *Mech. Dev.* **90**, 119-123.
Stern, C. D. and Vasiliauskas, D. (2000). Segmentation: a view from the border. *Curr. Top. Dev. Biol.* **47**, 107-129.
Strogatz, S. H. (1994). *Nonlinear Dynamics and Chaos*. Cambridge, Massachusetts: Westview.
Takke, C. and Campos-Ortega, J. A. (1999). her1, a zebrafish pair-rule like gene, acts downstream of notch signalling to control somite development. *Development* **126**, 3005-3014.
Terry, A. J., Sturrock, M., Dale, J. K., Maroto, M. and Chaplain, M. A. J. (2011). A spatio-temporal model of Notch signalling in the zebrafish segmentation clock: conditions for synchronised oscillatory dynamics. *PLoS ONE* **6**, e16980.
Trofka, A., Schwendinger-Schreck, J., Brend, T., Pontius, W., Emonet, T. and Holley, S. A. (2012). The Her7 node modulates the network topology of the zebrafish segmentation clock via sequestration of the Hes6 hub. *Development* **139**, 940-947.
Wright, G. J., Giudicelli, F., Soza-Ried, C., Hanisch, A., Ariza-McNaughton, L. and Lewis, J. (2011). DeltaC and DeltaD interact as Notch ligands in the zebrafish segmentation clock. *Development* **138**, 2947-2956.